# Design of Robot Gripper Jaws Based on Trapezoidal Modules [1]

Tao Zhang and Ken Goldberg[2]

IEOR Dept., UC Berkeley

**ABSTRACT**

*Assembly line reliability can be increased if grippers are carefully designed to capture and align parts. Jaw design depends on the geometric and mechanical properties of the part as well as its desired orientation. In this paper we propose a class of modular jaws based on rapidly machineable trapezoidal modules. An optimal jaw design is an arrangement of trapezoidal jaw modules that maximizes contacts between the gripper and the part at its desired final orientation over the constraints that: the jaws will capture and rotate the part to its desired orientation and achieve a form-closure grasp. Given the n-sided 2D convex projection of an extruded polygonal part, we develop an implemented $O(n^5)$ algorithm to find the optimal jaw design. The algorithm combines toppling, jamming, liftoff, accessibility, and form-closure analysis. We verify resulting designs by physical experiments.*

## 1    INTRODUCTION

*Grippers can be the most design-intensive components of an assembly system* [10]. Although grippers are widely used for automated manufacturing, assembly, and packing, the design of gripper jaws is usually ad-hoc and can be a major limiting factor in automated assembly.

Causey and Quinn [7] propose guidelines for the design of grippers in manufacturing. Based upon these criteria, we propose a modular approach where the standard parallel-jaw gripper is augmented with trapezoidal jaw modules.
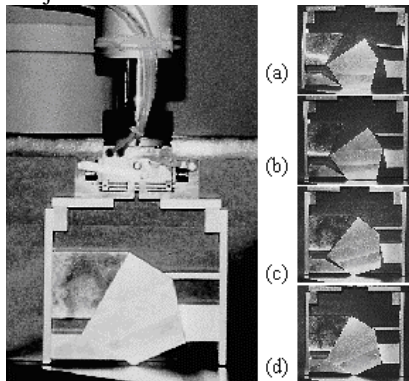


Figure 1 Gripper jaws align the part for assembly: (a) pushing (beginning); (b) pushing (ending); (c) toppling; and (d) fixturing.

As illustrated in Figure 1, the part is initially in the resting pose (a). It is necessary to rotate the part to the desired final orientation (d) for assembly. The idea is to design the gripper jaws so as to align the part as it is acquired. We divide the grasp into three phases: *pushing*, *toppling* and *fixturing*. Initially, one jaw makes contact with the part (the "pushing contact"). The jaw pushes the part along the work-surface until the part makes contact with the "toppling contact" on the second jaw. At this point the part begins to rotate (topple) from its initial orientation to the desired orientation. During toppling, the part is constrained by two contacts and the surface. When the part reaches its final fixtured orientation other jaw surfaces stop its motion. The optimal jaw design guides the part through these phases, avoids premature toppling, jamming, and liftoff, and fixtures the part in form closure with maximal linear contact.

## 2    RELATED WORK

There is a substantial body of research on robotic grasping; Bicchi and Kumar provide a concise survey in [3].

A number of papers consider part motion in the horizontal plane and how it can be used to reduce uncertainty. The motion of parts during grasp acquisition was first analyzed by Mason [13], who studies push mechanics as a role of passive compliance in grasping and manipulation. Erdmann and Mason [8] explore the use of motion strategies to reduce uncertainty in the location of objects. They described a systematic algorithm for sensorless manipulation to orient parts using a tilting tray. Brost [5] applies Mason's Rule to analyze the mechanics of the parallel-jaw gripper and polygonal parts. He shows that it is possible to align parts using passive push and squeeze mechanics. Goldberg [9] demonstrates that a modified parallel-jaw gripper could orient polygons up to symmetry by a sequence of normal pushes. Akella *et al.* [2] study a minimalist manipulation method to feed planar parts using a one joint robot over a conveyor belt.

Several authors address motion of parts in the vertical (gravitational) plane during grasping. Trinkle and Paul [16] show how to align parts in the gravitational plane by lifting them off work-surface using a planar gripper with two pivoting jaws. The pre-liftoff phase analysis of their paper is related to our toppling analysis. They generated *liftability regions* corresponding to contact that cause the part to: slide, jam, and break contact with the work-surface. We focus on design of jaw shape and show that parts can be rotated using only translational jaw motion. Abell and Erdmann [1] study how a planar

[2] For further information please contact goldberg@ieor.berkeley.edu.

polygon can be rotated while stably supported by two frictionless contacts. Rao *et al.* [15] give a planar analysis for picking up polyhedral parts using 2 hard-point contacts with a pivoting bearing, allowing the part to pivot under gravity to rotate into a new configuration. Blind *et al.* [4] present a "*Pachinko*"-like device to orient polygonal parts in the vertical plane. It consists of a grid of retractable pins that are programmed to bring the part to a desired orientation as the part falls.

Wallack and Canny [19] develop an algorithm for planning planar grasp configurations using a modular vise. Brown and Brost [6] turn the vise upside down and invent a modular parallel-jaw gripper. Each jaw consists of a regular grid of precisely positioned holes. By properly locating (inserting) four pins on each grid, the object can be grasped reliably at the desired orientation.

Mathematical programming has been employed to analyze grasping properties. Trinkle [16] introduced a nonlinear programming (NLP) model to predict instantaneous contact force, contact type, and velocity of grasped parts. The model minimizes the power generated by friction and gravity subject to kinematic constraints. Trinkle solves the problem using the primal-dual relationship. And shows that the problem can be reduced to a LP problem if the contacts are frictionless [17,18].

Our work is also motivated by recent research in toppling manipulation. Lynch [11,12] derived sufficient mechanical conditions for toppling parts in term of constraints on contact friction, location, and motion and we built on his analysis. Zhang and Gupta [21] study how parts can be reoriented as they fall down a series of steps. They derive the critical transition height, which is the minimum step height to topple a part from a given stable orientation to another. Yu *et al.* [20] estimate the mass and COM of objects by toppling. In [22], we introduced the toppling graph to geometrically represent the mechanics of toppling. We extended toppling analysis to parallel-jaw grasping with point contacts in [23]. In the current paper, we consider non-point contacts and solve for optimal jaws based on trapezoidal modules.

## 3 DESIGN PROBLEM DEFINITION

We assume the part can be treated as a rigid extrusion of a polygon; both the part and the jaws are rigid; part geometry and location of the COM and the jaws are known; part motion is sufficiently slow to apply quasi-static analysis.

We consider the following design problem. The input is the *n*-sided convex projection of an extruded polygonal part, its COM, its initial and desired orientations, $e$ vertex clearance radius, $m_t$, $m_s$ friction coefficients between gripper-part and part-surface, respectively. The output is a pair of gripper jaws, each specified by a list of trapezoidal modules.

Figure 1 illustrates an optimal solution. Without loss of generality, we assume the part rotates counterclockwise. Each jaw consists of a vertical base-plate and a set of trapezoidal modules arranged on the base-plate. To facilitate jaw machining and installation, we consider a class of trapezoidal jaw modules. Each jaw module is determined by the locations of two vertices that make contact with the part. The line segment between these two vertices represents an *accessible segment* on an edge of the part at its desired orientation. The objective is to find the set of accessible segments with maximum total length.

We can define the problem, called OPTIMIZE-JAWS, using a nonlinear programming model:

*max*:  total length of linear contact area between part and gripper at desired orientation
*s. t.*:  1. pushing is successful;
    2. toppling is successful;
    3. no jamming occurs;
    4. no liftoff occurs;
    5. no collisions on part motion trajectory;
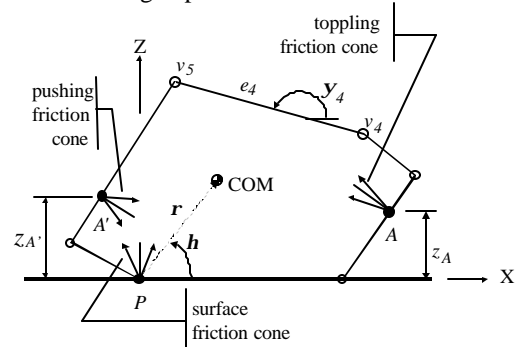    6. final grasp is secure.



**Figure 2** Notation.

As shown in Figure 2, the part sits on a flat work-surface at a stable initial orientation. We define the World frame, *W*, to be a Cartesian coordinate system originating at pivot point *P* with X-axis on the surface pointing right, Z-axis vertical to the surface pointing up.

The COM is a distance *r* from the origin and angle *h* from the +X direction at its initial orientation. The pushing contact, *A'*, is a distance $z_{A'}$ from the surface; the toppling contact, *A*, is a distance $z_A$ from the surface.

Starting from the pivot, we consider each edge of the part in counter-clockwise order, namely $e_1$, $e_2$, …, $e_n$. The edge $e_i$, with vertices $v_i$ at $(x_i, z_i)$ and $v_{(i+1)}$ at $(x_{(i+1)}, z_{(i+1)})$, is in direction $y_i$ from the X-axis. The surface friction cone half-angle is $a_s = \tan^{-1} m_s$ and the toppling (pushing) friction cone half-angle is $a_t = \tan^{-1} m_t$

Let $F_t$, $F_p$, and $F_s$ denote the contact force at *A*, *A'*, and the surface, respectively, and $f_t$, $f_p$, and $f_s$ denote the direction of the corresponding contact force. We also denote the direction at the left edge of

the toppling (/ pushing / surface) friction cone as $f_{tl}$ (/$f_{pl}$ / $f_{sl}$) and the right edge as $f_{tr}$ (/$f_{pr}$ / $f_{sr}$). Let $f_g$ denote the vertical line through the part's COM. Let $_aI_b$ denote the intersection of line $a$ and line $b$, where $a$ and $b$ can be anyone of $f_{tl}, f_{pl}, f_{sl}, f_{tr}, f_{pr}, f_{sr}, f_g, f_t, f_p,$ and $f_s$.

Let $\boldsymbol{q}$ denote the rotation angle of the part; initially $\boldsymbol{q} = 0$ and finally $\boldsymbol{q} = \boldsymbol{q}_l$. Let $\boldsymbol{q}$ denote the rotation angle where the COM is right above $P$; therefore, $\boldsymbol{q} = \pi/2 - \boldsymbol{h}$ We partition edge $e_i$ by $w_i$ that is the distance from vertex $v_i$. Therefore, a point on $e_i$ can be expressed as $(x_i + w_i \cos \boldsymbol{y}_i, z_i + w_i \sin \boldsymbol{y}_i)$.

We say an edge $e_k$ is *visible* if it can be seen from +X direction; *invisible*, otherwise. Therefore, $e_k$ is visible if $0 < \boldsymbol{y}_k + \boldsymbol{q} < \pi$; $e_k$ is *invisible* if $\pi < \boldsymbol{y}_k + \boldsymbol{q} < 2\pi$. Notice that $A$ can only make contact with visible edges and $A'$ with invisible edges.

## 4 ALGORITHM

We develop a numerical algorithm to find the optimal jaw design. The algorithm is based on an efficient enumeration of feasible designs that exploits part geometry and a graphical force analysis.

The feasible region for the optimization problem is a curve plane defined by $(z_A, z_{A'}, L)$, where $L$ is a function of $(z_A, z_{A'})$ and represents the total contact length between the part and the gripper at the desired final orientation. We approximate the maximal (optimal) point of this plane by sampling the plane.

### 4.1 Location of Contacts

The contacts could switch edges as the part rolls. Therefore, we have to check which edge the contacts keep touch with at the different part rotation angle $\boldsymbol{q}$

We first consider the location of $A'$. It keeps touch with a invisible edge $e_k$ at $\boldsymbol{q}$ if $x_k \sin \boldsymbol{q} + z_k \cos \boldsymbol{q} > z_{A'} > x_{k+1} \sin \boldsymbol{q} + z_{k+1} \cos \boldsymbol{q}$

Therefore, we can find the corresponding $x_{A'}$ by:

$$x_{A'} = x_k \cos \boldsymbol{q} - z_k \sin \boldsymbol{q} + \frac{z_{A'} - x_k \sin \boldsymbol{q} - z_k \cos \boldsymbol{q}}{\tan(\boldsymbol{y}_k + \boldsymbol{q})} . \quad \#1$$

The location of the toppling contact $(x_A, z_A)$ can be derived in a similar way [24].

### 4.2 Pushing Constraints

To guarantee the linear translation of the part on the surface during pushing, neither toppling nor jamming could occur.

To eliminate the pushing contact that may result in jamming, $F_p$ should overcome the friction between the part and the surface. By static analysis,

$$\boldsymbol{w} = \boldsymbol{y}_i + \boldsymbol{p}/2 \pm \boldsymbol{a} \qquad \#2$$
$$Mg - F_p \sin \boldsymbol{w} = N \qquad \#3$$
$$F_p \cos \boldsymbol{w} \geq \boldsymbol{m}_s N \qquad \#4$$

Therefore, we have:

$$\cos \boldsymbol{w} + \boldsymbol{m}\sin \boldsymbol{w} \geq \frac{\boldsymbol{m}_s Mg}{F_p} \qquad \#5$$

Since $\cos \boldsymbol{w} \geq 0$ and $\dfrac{\boldsymbol{m}_s Mg}{F_p} \geq 0$, then:

$$1 + \boldsymbol{m}_s \tan \boldsymbol{w} \geq 0$$
$$\Rightarrow \tan(\boldsymbol{y}_i + \frac{\boldsymbol{p}}{2} \pm \boldsymbol{a}_t) \geq -\frac{1}{\boldsymbol{m}_s} \qquad \#6$$
$$or \quad \boldsymbol{y}_i \geq \frac{3\boldsymbol{p}}{2}$$

Therefore, given the pushing contact makes contact with edge $e_i$, to guarantee no jamming equation #6 must be satisfied.
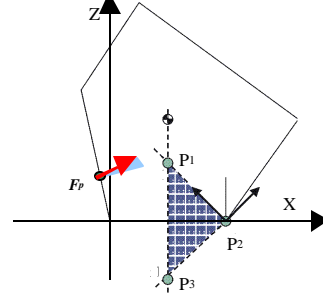


**Figure 3** Condition to prevent toppling.

To prevent the part from toppling during the pushing phase, we begin by constructing a Lynch-like triangle with vertices $P_1$, $P_2$, and $P_3$ as shown in Figure 4. $P_1(x_{p1}, z_{p1})$ is $_gI_{sl}$, $P_2(x_{p2}, z_{p2})$ is $P$, and $P_3(x_{p3}, z_{p3})$ is $_gI_{sr}$. From these definitions we have:

$$x_{p1} = s, \qquad \#7$$
$$z_{p1} = (x_2 - s)/\boldsymbol{m}, \qquad \#8$$
$$x_{p2} = 0, \qquad \#9$$
$$z_{p2} = x_2, \qquad \#10$$
$$x_{p3} = s, \qquad \#11$$
$$z_{p3} = -(x_2 - s)/\boldsymbol{m}, \qquad \#12$$
where $s = \boldsymbol{r}\cos \boldsymbol{h} \qquad \#13$

To guarantee the pushing contact does not roll the part clockwise, every force in the pushing friction cone must not make a positive moment (i.e., the contact force passes around the triangle in a clockwise fashion.) respect to the $P_1P_2P_3$ triangle [14]. Therefore, $f_{pl}$ must pass below the highest vertex of the triangle.

Let $_1w_i$ denote the edge contact on $e_i$ where $f_{pl}$ passes exactly through point $P_1$. We find $_1w_i$ by projecting a line from $P_1$ at the angle of $f_{pl}$ until it intersects the edge of the part:

$_1w_i = (z_i - (x_2 - s)/\boldsymbol{m} - (x_i - s) \tan \boldsymbol{b}_l) / (\cos \boldsymbol{y}_i \tan \boldsymbol{b}_l - \sin \boldsymbol{y}_i), \qquad \#14$

where $\boldsymbol{b}_l = \boldsymbol{y}_i + \boldsymbol{p}/2 + \boldsymbol{a}$.

The contacts for $f_{pl}$ passing through $P_2$ and $P_3$ are given by:

$_2w_i = (z_i - x_2 - x_i \tan \boldsymbol{b}_l) / (\cos \boldsymbol{y}_i \tan \boldsymbol{b}_l - \sin \boldsymbol{y}_i), \#15$
$_3w_i = (z_i + (x_2 - s)/\boldsymbol{m} - (x_i - s) \tan \boldsymbol{b}_l) / (\cos \boldsymbol{y}_i \tan \boldsymbol{b}_l - \sin \boldsymbol{y}_i). \qquad \#16$

To guarantee the pushing contact on an edge $e_i$ cannot roll the part clockwise, the following inequality must be satisfied:

$$_i z_{A'} < D_{Hi} = z_i + w_{Hi} \sin \boldsymbol{y}_i, \qquad \#17$$

where $w_{Hi} = \begin{cases} {}_1w_i & y_i \geq p - a_i + a_s \\ {}_2w_i & p - a_i + a_s \geq y_i \end{cases}$ that is the minimum of ${}_1w_i$, ${}_2w_i$, and ${}_3w_i$.

Similarly, to guarantee the pushing contact does not roll the part counter-clockwise, the following inequality must be satisfied:

$$_iz_{A'} > D_{Li} = z_i + w_{Li}\sin y_i, \qquad \#18$$

where $b_r = y_i + p/2 - a_i$ and $w_{Li} = \begin{cases} {}_2w_i & y_i \geq 2p + a_i - a_s \\ {}_3w_i & 2p + a_i - a_s \geq y_i \end{cases}$ that is the maximum of ${}_1w_i$, ${}_2w_i$, and ${}_3w_i$.

In summary, to guarantee linear translation of the part without toppling and jamming, inequality #6, #17, and #18 must be satisfied if the pushing contact makes contact with edge $e_i$.

## 4.3 Toppling Constraints

During toppling, the part rotates about $P$. The system of forces on the part: $F_p, F_t, F_s$, and the part's weight $Mg$, must generate a negative moment on the part with respective to $P$. The contact forces lie on the edge of the corresponding friction cones. Since $P$ slides to the right, the contact force from the surface is on the direction of $f_{sl}$. $F_t$ is on the direction of $f_{tl}$ if $x_A > 0$; $f_{tr}$ if $x_A < 0$. $F_p$ is on the direction of $f_{pr}$ if $x_{A'} > 0$; $f_{pl}$ if $x_{A'} < 0$ [24].

Given the part stays on the surface and the height of $A'$, the toppling function [23], $H_j(q)$, is the minimum height at $q$ that $A$ in contact with edge $e_j$ must be in order to roll the part instantaneously, where $q = 0 \sim q_l$ during toppling.

Consider an area in $W$ defined by linear edges. Let a *toppling area* denote an area such that toppling is guaranteed if $F_t$ makes a negative moment about every point in the area. When $q < q_l$, there only exists a toppling area. We derive the toppling function depending on the direction of $F_p$, i.e., $x_{A'} > 0$ or $x_{A'} < 0$ (see [24] for details).

## 4.4 Jamming Constraints

The part continues to rotate after it has reached $q_l$, and jamming may occur due to friction.

Given the part stays on the surface and the height of $A'$, the jamming function [23], $J_j(q)$, is the minimum height at $q$ that $A$ in contact with edge $e_j$ must be in order to guarantee no jamming.

Let a *jamming area* denote an area such that no jamming is guaranteed if $F_t$ does not make a positive moment about every point in the area. We consider the jamming function by investigating the location of $A'$. We divide quadrant II of $W$ into four zones by $f_g$ and $f_{sl}$. Therefore, $A'$ must lie in one of these zones during toppling.

We first check which zone $A'$ belongs to at $q$. Then we check if there exists a jamming area or a toppling area. Finally, we derive the jamming function if a jamming area exists and the toppling function if a toppling area exists (see [24] for details).

## 4.5 Liftoff Constraints

As the part rotates, it may be lifted off from the surface. We now find the condition that insures the contact between the part and the surface.

In rolling phase, we only need to consider the cases where: $y_i > p + a_i - a_s$ if $x_{A'} < 0$; or $y_i > p + a_i + a_s$ if $x_{A'} > 0$ because there is no toppling area otherwise. In these cases, the part keeps contact with the surface if and only if $F_t$ makes negative moment about the line segment between $_gI_p$ and $_pI_s$ [24]. Therefore, the toppling constraints include the non-liftoff conditions when $q < q_l$.

When $q > q_l$, we assume the part is just about to be lifted off from the surface if a jamming area exists. Therefore, we have:

$$F_p \cos a_i + F_t \cos a_j = 0, \qquad \#19$$

where $a_i = \begin{cases} b_{il} & if\ x_{A'} < 0 \\ b_{ir} & if\ x_{A'} > 0 \end{cases}$ and $a_j = \begin{cases} b_{jl} & if\ x_A > 0 \\ b_{jr} & if\ x_A < 0 \end{cases}$.

To guarantee non-liftoff, forces must satisfy:

$$F_p \sin a_i + F_t \sin a_j - G < 0, \qquad \#20$$

Therefore, $\tan a_i - \tan a_j < 0$.

Notice that when both $F_p$ and $F_t$ point down, i.e. $\pi < a_i < 2\pi$ and $\pi < a_j < 2\pi$, the inequality is always true; when both $F_p$ and $F_t$ point up, i.e. $2\pi < a_i < 3\pi$ and $0 < a_j < \pi$, the inequality is always false.

## 4.6 Toppling Graph

Our analysis involves the graphical construction of a set of functions. All of these functions are piecewise sinusoidal and dependent on $q$. They map from part orientation to height: $S^1 \to \hat{\mathbf{A}}^+$, where $S^1$ is the set of planar orientations. The functions include vertex functions, toppling functions, and jamming functions. The toppling graph [22], which consists of these functions, helps us to identify the range of the contact permits toppling.

## 4.7 Trajectory Analysis

Once the part has been toppled to $q_l$, the jaws must stop the part's rotation and securely hold it. We want to maximize the contact between the part and the jaws for the most robust performance.

During toppling, the part is constrained by two contacts and the surface. We first consider the motion trajectory of the visible edges. We take the toppling contact as a fixed point; therefore, the part motion is constrained by $A$ and the surface (see Figure 4). The motion trajectory of the invisible edges can be obtained by the same method taking $A'$ as a fixed point; therefore, the part motion is constrained by $A'$ and the surface.

The part performs both rotation and linear translation during toppling. We decompose the part motion into pure rotation and pure linear translation. The part first rotates about $P$ to *semi-position*, and then translates to *actual-position*. Let $(_q x_j, {}_q z_j)$ and $(_q x'_j, {}_q z'_j)$ denote the actual-position and the semi-position of vertex $v_j$ after the part is toppled by $q$

respectively. Let $(_d x_j, {}_d z_j)$ and $(_d x'_j, {}_d z'_j)$ denote the actual-position and the semi-position of vertex $v_j$ after the part is toppled to its desired orientation, respectively. Let $_q x_t$ and $_d x_t$ denote the distance between the actual-position and the semi-position of any point after the part is toppled by $\boldsymbol{q}$ and $\boldsymbol{q}_t$, respectively.

No obstacle (any portion of the jaws) can block the motion trajectory of the part during toppling. We developed *quasi-vertex functions* to represent the motion trajectory of vertices. Given $z_A$, the quasi-vertex function $Q_{jk}(\boldsymbol{q}\ z_A)$ indicates the location of $v_k$ in $F_j$ as the part rotates.
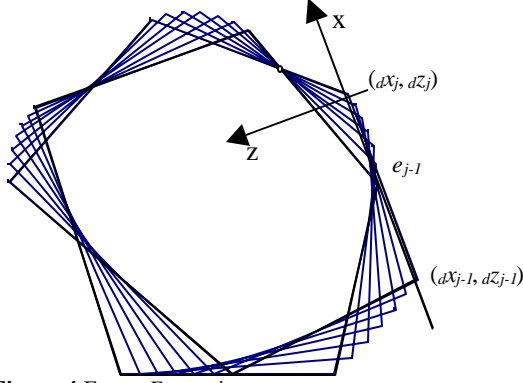
**Figure 4** Frame $F_j$ notation.

We define a frame of reference $F_j$ at the desired orientation of the part. As shown in Figure 5, $F_j$ originates at $v_j$. The Z-axis of $F_j$ is the interior normal of edge $e_{(j-1)}$, and the X-axis is on edge $e_{(j-1)}$ obeying the right-hand rule. We obtain $Q_{jk}(\boldsymbol{q}\ z_A)$ by transforming the motion trajectory of $v_k$ in $W$ to $F_j$.

We know that $_d x_t = {}_d x_A - {}_d x'_A$, where $_d x_A = x_A$ since $A$ is fixed. $A$ makes contact with edge $e_m$ if $_d z'_m < z_A < {}_d z'_{m+1}$. Therefore, we can find $_d x'_A$, and then we obtain:

$$_d x_t = x_A - \frac{(z_A - {}_d z'_m)({}_d x'_{m+1} - {}_d x'_m)}{_d z'_{m+1} - {}_d z'_m} - {}_d x'_m.\ \#\ 21$$

So the transformation matrix $^{Fj}T_W$ is given by:
$$^{Fj}T_W = [^W T_{Fj}]^{-1} =$$

$$\begin{bmatrix} \cos(\boldsymbol{y}_{j-1}+\boldsymbol{q}_d) & 0 & \sin(\boldsymbol{y}_{j-1}+\boldsymbol{q}_d) & -(_d x'_j + {}_d x_t)\cos(\boldsymbol{y}_{j-1}+\boldsymbol{q}_d) - {}_d z'_j \sin(\boldsymbol{y}_{j-1}+\boldsymbol{q}_d) \\ 0 & 1 & 0 & 0 \\ -\sin(\boldsymbol{y}_{j-1}+\boldsymbol{q}_d) & 0 & \cos(\boldsymbol{y}_{j-1}+\boldsymbol{q}_d) & +(_d x'_j + {}_d x_t)\sin(\boldsymbol{y}_{j-1}+\boldsymbol{q}_d) - {}_d z'_j \cos(\boldsymbol{y}_{j-1}+\boldsymbol{q}_d) \\ 0 & 0 & 0 & 1 \end{bmatrix}$$

$$\#\ 22$$

We next describe the motion trajectory of vertex $v_k$ in $W$ numerically. At each sampling $\boldsymbol{q}$ we compute the position of $v_k$:

$$V_W = \begin{bmatrix} x_k \cos\boldsymbol{q} - z_k \sin\boldsymbol{q} + {}_q x_t \\ 0 \\ x_k \sin\boldsymbol{q} + z_k \cos\boldsymbol{q} \\ 1 \end{bmatrix}, \qquad \#\ 23$$

where $_q x_t = x_A - \dfrac{(z_A - {}_q z'_l)({}_q x'_{l+1} - {}_q x'_l)}{_q z'_{l+1} - {}_q z'_l} - {}_q x'_l$ if $_q z'_l < z_A < {}_q z'_{l+1}$. Thus, quasi-vertex function $Q_{jk}(\boldsymbol{q}\ z_A)$ for vertex $v_k$ can be shown to be:

$$Q_{jk}(\boldsymbol{q}) = \begin{bmatrix} _x Q_{jk}(\boldsymbol{q}, z_A) \\ _z Q_{jk}(\boldsymbol{q}, z_A) \end{bmatrix}$$

$$= \begin{bmatrix} (_q x'_k - {}_d x'_j + {}_q x_t - {}_d x_t)\cos(\boldsymbol{y}_{j-1}+\boldsymbol{q}_d) + (_q z'_k - {}_d z'_j)\sin(\boldsymbol{y}_{j-1}+\boldsymbol{q}_t) \\ -(_q x'_k - {}_d x'_j + {}_q x_t - {}_d x_t)\sin(\boldsymbol{y}_{j-1}+\boldsymbol{q}_d) + (_q z'_k - {}_d z'_j)\cos(\boldsymbol{y}_{j-1}+\boldsymbol{q}_d) \end{bmatrix}$$

$$\#\ 24$$

The line segment, connecting two corresponding points of $Q_{jk}(\boldsymbol{q}\ z_A)$ and $Q_{j(k+1)}(\boldsymbol{q}\ z_A)$ at the same rotation angle, represents the configuration of edge $e_k$ in $F_j$. We denote it by the quasi-edge function $E_{jk}(\boldsymbol{q}\ z_A)$. Figure 5 illustrates $Q_{43}(\boldsymbol{q}\ z_A)$ and $Q_{44}(\boldsymbol{q}\ z_A)$, and $E_{43}(\boldsymbol{q}\ z_A)$ for the sample part given $z_{A'} = 0.5$cm and $z_A = 3.65$cm.
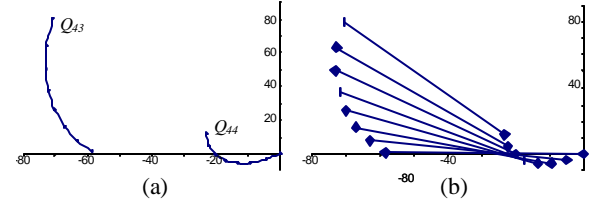
**Figure 5** Quasi-vertex functions (a) and quasi-edge functions (b).

We obtain an accessibility graph of $F_j$ by combining $Q_{jk}(\boldsymbol{q}\ z_A)$'s for all the visible vertices $v_k$'s into one graph. We say a portion of an edge is an *accessible segment* if the gripper can contact this portion at the desired final orientation of the part without blocking its motion trajectory. Therefore, the portion of edge $e_{(j-1)}$ is accessible if there is no intersection between the quasi-edge functions and this portion of X-axis in the accessibility graph of $F_j$. Figure 5 illustrates the accessibility graph of $F_4$ based on the sample part given $z_{A'} = 0.5$cm and $z_A = 3.65$cm.
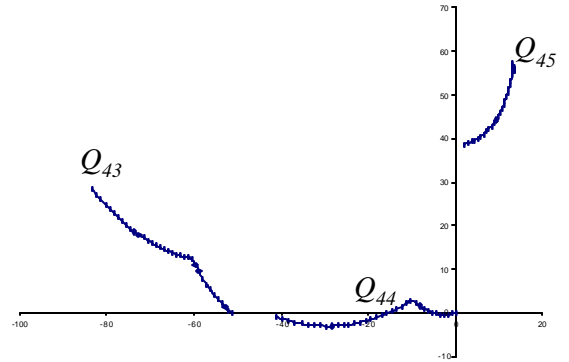
**Figure 6** The accessibility graph of $F_4$.

Starting from any point of $Q_{jk}(\boldsymbol{q}\ z_A)$'s in the accessibility graph of $F_j$ with $_z Q_{jk}(\boldsymbol{q}\ z_A) < 0$, we search the trajectory of $e_k$ and the neighbor edges recursively to find all the intersections between the corresponding quasi-edge functions and X-axis. We obtain the accessible segment on edge $e_{(j-1)}$ by eliminating those intersections. Repeating this

analysis on all the edges of the part, we get the set of accessible segments for the pair of ($z_A$, $z_{A'}$).

Additionally, we require the jaws to achieve a form-closure grasp on the part. It is well known that to check the form-closure grasps is equivalent to solving a system of equations [18]. We find the optimal design by ranking the form-closure check survivors based upon the total length of contact. Figure 7 demonstrates the optimal design with maximal $L$ for the sample part where $z_{A'} = 0.5$cm and $z_A = 22.6$cm.
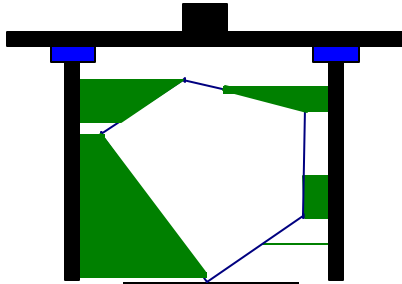


**Figure 7** An example: the optimal jaw design.

Given the $n$-sided convex projection of an extruded polygonal part, our algorithm takes $O(n^2)$ to find a pair of feasible ($z_A$, $z_{A'}$). For each ($z_A$, $z_{A'}$), we apply $O(n^3)$ time trajectory analysis to find the set of the accessible segments. Therefore, the running time is $O(n^5)$.

## 5. IMPLEMENTATION RESULTS

We conducted a physical experiment using an AdeptOne industrial robot and a parallel-jaw gripper with jaws designed using the methodology described in this paper. The part and the jaws were machined from aluminum. The corresponding friction cone half angles are $a_t = 5° \pm 2°$, and $a_p = 5° \pm 2°$.

As illustrated in Figure 1, the part begins at stable orientation (a). Its desired orientation (d) for assembly is at $q = 25°$. We choose $A$ and $A'$ at $z_A = 5.5$cm and $z_{A'} = 0.4$cm, respectively. The analysis yields the optimal jaw design with $L = 16.2$cm.

## 6. DISCUSSION AND FUTURE WORK

Gripper jaw design has been ad-hoc and particularly challenging when the part's natural resting pose differs from the desired grip/insertion pose. In this paper we describe a new approach to this problem where the gripper jaws guide the part into alignment and achieve the maximal linear contact with the part at its desired orientation.

Our next objective is to validate performance of the modular jaw designs in terms of reliability and variation in shape, mass distribution, and friction. We will then extend the approach to non-extruded 3D parts.

## REFERENCES

[1]    T. Abell and M. Erdmann. "Stably supported rotations of a planar polygon with two frictionless Contacts," in *Proc. IEEE/RSJ Int. Conf. Intell. Robots Syst.*, Pittsburgh, 1995, pp. 411-418.

[2]    S. Akella, W. Huang, K. Lynch, and M. Mason. "Parts feeding on a conveyor with a one joint robot," *Algorithmica*, Vol.26, No.3-4, pp. 313-344, 2000.

[3]    A. Bicchi and V. Kumar. "Robotic grasping and contact: a review," in *Proc. 2000 IEEE Int. Conf. Robot. Automat.*, San Francisco, 2000, pp. 348-353.

[4]    S. Blind, C. McCullough, S. Akella, and J. Ponce. "A reconfigurable parts feeder with an array of pin," in *IEEE Int. Conf. Robot. Automat.*, San Francisco, 2000, pp. 147-153.

[5]    R. Brost. "Automatic grasping planning in the presence of uncertainty," *Int. J. Robot. Automat.*, Vol. 7, No. 1, pp. 3-17, 1988.

[6]    Brown, R., and R. Brost. "A 3-D modular gripper design tool," *IEEE Trans. Robot. Automat.*, Vol. 15, No. 1, pp. 174-186, 1999.

[7]    G. Causey and R. Quinn. "Gripper design guidelines for modular manufacturing," in *IEEE Int. Con. Robot. Automat.*, Leuven, Belgium, 1998, pp. 1453-1458.

[8]    M. Erdmann and M. Mason. "An exploration of sensorless manipulation," *IEEE J. Robot. Automat.*, vol. 4, no. 4, 1988, pp. 369-379.

[9]    K. Goldberg. "Orienting polygonal parts without sensors," *Algorithmica*, *Special Issue: Computational Robotics*, vol. 10, no. 2, pp. 201-225, 1993.

[10]    W. Hessler. "How to build simple, effective pick-and-place devices," *Robot Today*, vol. 9, no. 4, pp. 1-5, 1996.

[11]    K. Lynch. "Toppling manipulation," in *IEEE Int. Con. Robot. Automat.*, Detroit, 1999, pp. 2551-2557.

[12]    K. Lynch. "Inexpensive conveyor-based parts feeding," *Assembly Automat.*, vol. 19, no. 3, pp. 209-215, 1999.

[13]    M. Mason and J. Salisbury. *Robotic Hands and the Mechanics of Manipulation*, Boston, MA: MIT, 1985.

[14]    M. T. Mason. "Two graphical methods for planar contact problems," in *IEEE/RSJ Int. Workshop Intell. Robots Syst.*, Osaka, Japan, 1991, pp. 443-448.

[15]    A. Rao, D. Kriegman and K. Goldberg. "Complete algorithm for feeding polyhedral parts using pivot grasps," *IEEE Trans. Robot. Automat.*, vol. 12, no. 2, pp. 331-342, 1996.

[16]    J. Trinkle and R. Paul. "Planning for dexterous manipulation with sliding contacts," *Int. J. Robot. Res.*, vol. 9, no. 3, pp. 24-48, 1990.

[17]    J. Trinkle. "On the stability and instantaneous velocity of grasped frictionless objects," *IEEE Trans. Robot. Automat.*, vol. 8, no. 5, pp. 560-572, 1992.

[18]    J. Trinkle. "A quantitative test for form closure grasps," in *IEEE Int. Conf. Intell. Robots Syst.*, Raleigh, 1992, pp. 1670-1677.

[19]    A. Wallack and J. Canny. "Planning for modular and hybrid fixtures," *Algorithmica*, vol. 19, no. 1-2, pp. 40-60, 1997.

[20]    Y. Yu, K. Fukuda and S. Tsujio. "Estimation of mass and center of mass of graspless and shape-unknown object," in *IEEE Int. Con. Robot. Automat.*, Detroit, 1999, pp. 2893-2898.

[21]    R. Zhang and K. Gupta. "Automatic orienting of polyhedral through step devices," in *IEEE Int. Con. Robot. Automat.*, Leuven, Belgium, 1998, pp. 550-556.

[22]    T. Zhang, G. Smith, R. Berretty, M. Overmars, and K. Goldberg. "The toppling graph: designing pin sequences for part feeding," in *IEEE Int. Con. Robot. Automat.*, San Francisco, 2000, pp. 139-146.

[23]    T. Zhang, G. Smith and K. Goldberg. "Compensatory grasping with the parallel-jaw gripper," in *4th Int. Workshop Algorithmic Foundations Robot.*, Hanover, NH, 2000.

[24]    T. Zhang and K. Goldberg. "Optimal Design of Robot Gripper Jaws," Tech. Rep. 00-2, ALPHA lab, UC Berkeley, 2000.